

PROCEEDINGS OF SPIE

SPIDigitalLibrary.org/conference-proceedings-of-spie

Multi-wavelength time-lens source and its application to nonresonant background suppression for coherent anti-Stokes Raman scattering microscopy

Bo Li, Kriti Charan, Ke Wang, David Sinefeld, Chris Xu

Bo Li, Kriti Charan, Ke Wang, David Sinefeld, Chris Xu, "Multi-wavelength time-lens source and its application to nonresonant background suppression for coherent anti-Stokes Raman scattering microscopy," Proc. SPIE 10069, Multiphoton Microscopy in the Biomedical Sciences XVII, 100690Y (21 February 2017); doi: 10.1117/12.2250347

SPIE.

Event: SPIE BiOS, 2017, San Francisco, California, United States

Multi-wavelength time-lens source and its application to nonresonant background suppression for coherent anti-Stokes Raman scattering microscopy

Bo Li^{*a}, Kriti Charan^a, Ke Wang^b, David Sinefeld^a, Chris Xu^a

^aSchool of Applied and Engineering Physics, Cornell University, Ithaca, NY, USA 14853; ^bKey Laboratory of Optoelectronic Devices and Systems of Ministry of Education and Guangdong Province, College of Optoelectronic Engineering, Shenzhen University, Shenzhen, China 518060

ABSTRACT

We demonstrate a robust, all-fiber, two-wavelength time-lens source for background-free coherent anti-Stokes Raman scattering (CARS) imaging. The time-lens source generates two picosecond pulse trains simultaneously: one at 1064 nm and the other tunable between 1040 nm and 1075 nm (~ 400 mW for each wavelength). When synchronized to a mode-locked Ti:Sa laser, the two wavelengths are used to obtain on- and off-resonance CARS images. Real-time subtraction of the nonresonant background in the CARS image is achieved by the synchronization of the pixel clock and the time-lens source. Background-free CARS imaging of sebaceous glands in *ex vivo* mouse tissue is demonstrated.

Keywords: Ultrafast lasers; Fiber optics sources; Raman microscopy.

1. INTRODUCTION

Coherent anti-Stokes Raman scattering (CARS) allows label-free imaging of biological samples with endogenous image contrast based on vibrational spectroscopy [1, 2]. Despite these advantages, a major drawback of CARS is the existence of a nonresonant background, which obscures the contrast of the resonant CARS image. In practice, an image free of non-resonant background can be acquired by subtracting the off-resonance image from the on-resonance one, however, the on- and off-resonance images are typically acquired by tuning the wavelength of the Stokes laser, and the slow tuning speed inevitably introduces spectral artifacts due to sample motion in live cell or tissue imaging [3, 4]. This problem can be solved by using three synchronized lasers, which allow the simultaneous recording of on- and off-resonance images. Current three-color synchronized lasers for CARS imaging are realized by OPOs or synchronized mode-locked Ti:Sapphire laser, which are costly and difficult to implement in practice [5, 6].

In this paper, we demonstrate a robust, cost-effective, all-fiber, two-wavelength time lens source for background-free CARS imaging. The time-lens source generates two picosecond pulse trains simultaneously: one fixed at 1064 nm and the other tunable between 1040 nm and 1075 nm. The average power and pulse width for each wavelength are approximately 400 mW and 1.9 ps, respectively. When synchronized to a mode-locked Ti:Sapphire (Ti:Sa) laser, the two wavelengths are used to obtain on- and off-resonance CARS images. Real-time (pixel by pixel with pixel dwell time of ~ 2 μ s) subtraction of the nonresonant background in the CARS image is achieved by the synchronization of the microscope pixel clock and the time-lens source so that for each pixel in the acquired image the signal is excited by the pump and only one of the Stokes beams. Background-free CARS imaging of sebaceous glands in *ex vivo* mouse tissue is demonstrated. The demonstrated technique enables convenient synchronization to both the microscope pixel clock and the mode-locked laser in a robust, cost-effective, all-fiber configuration, and is scalable to include more wavelengths. Multi-wavelength time-lens source may provide an all-fiber, user-friendly alternative for background-free CARS imaging.

*bl627@cornell.edu;

2. EXPERIMENTS

2.1 Experimental setup

The experimental setup is shown in Figure 1. The pump for CARS imaging is obtained by pulse shaping the pulse from a femtosecond source. A mode-locked Ti:Sa laser (Mai Tai, Spectra-Physics) delivered femtosecond pulses with a duration of 100 fs at 80 MHz. The femtosecond pulse is sent through a pulse shaper. Using a slit in the Fourier plane, the femtosecond pulse is translated into a picosecond pulse [7].

The Stokes beams are generated from a two-wavelength time-lens source synchronized to the pump. A GaAs photodetector (ET-4000, EOT) detects a small portion of the output of the Ti:Sa mode-locked laser and generates a RF pulse train. The RF pulse train is then divided into two branches. One branch is filtered with a narrowband (NB) filter (with a 3dB bandwidth of 50 MHz) centered at the 125th harmonic of the 80 MHz repetition rate (i.e., 10 GHz). The resulting 10 GHz sinusoid is amplified to drive two electro-optic phase modulators (2PMs, EOSPACE) with an amplitude of $\sim 14 V_{pp}$ (V_{pp} is the peak-to-peak drive voltage) for each phase modulators. The other branch is amplified and is used to drive the Mach-Zehnder intensity modulator (IM, EOSPACE). The intensity modulator carves synchronized pulses onto the two CW sources, which consist a 1064 nm CW laser (QFBGLD-1060-30P, QPhotonics) and a wavelength-tunable CW laser (TEC-520-1060-100, Sacher Lasertechnik). The output pulses from the IM have temporal width of 80 ps due to the limited bandwidth of the components. A pair of transmission gratings (T-1600-1060s, LightSmyth) is used for dispersion compensation and pulse compression. The dispersion caused by the length of the fiber introduces a small, fixed walk-off between the pulses of the two wavelengths, which is compensated by using two separate mirrors in the compressor. We used Yb^{3+} doped fiber amplifiers (pre-amp) to compensate for the loss caused by the pulse carving and the phase modulators, and another Yb^{3+} doped fiber amplifiers (power amp) to increase the output power up to 800 mW. When both CW sources are modulated and present in the time-lens source, the average power per wavelength can reach up to 400 mW.

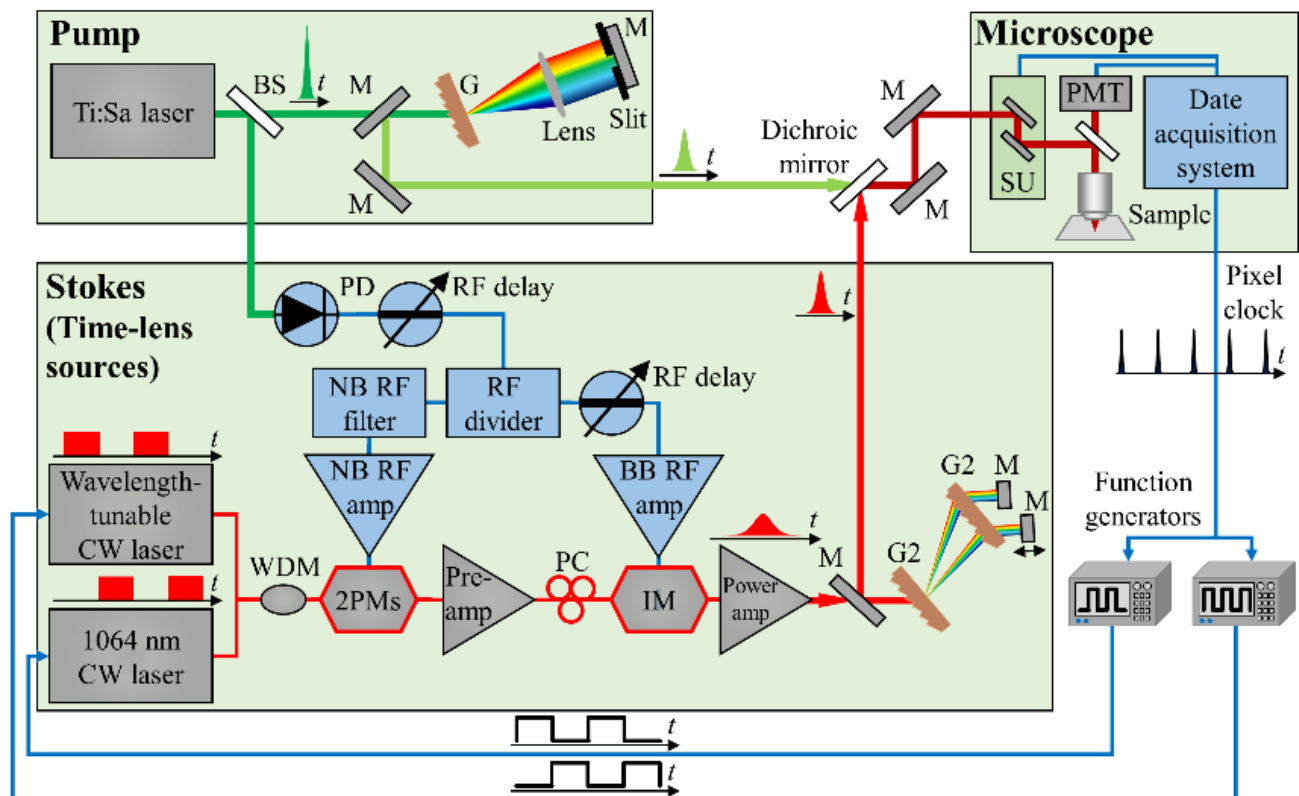


Figure 1. Experimental setup of the two-wavelength time-lens source (Stokes) synchronized to a mode-locked Ti:Sa laser (pump). BS, beam sampler; M, mirror; G, grating (T-1400-800s-2415-94, 1400 line/mm, Lightsmyth); SU, scanning unit; PMT, photomultiplier tube; NB, narrowband; BB, broadband; WDM, Wavelength-division multiplexer; PM, phase modulator; IM, intensity modulator; G2, grating (T-1600-1060s, 1600 line/mm, Lightsmyth).

2.2 Laser characterizations

Temporal synchronization between the pump and the Stokes is achieved by RF delay lines, which can be adjusted over a large range (~ 0.8 ns), eliminating the need for cumbersome mechanical optical delay lines. The pump, Stokes, and nonresonant Stokes beams are spatially combined with a dichroic mirror and sent into a laser-scanning microscope (FV1000MPE, Olympus) with a 20x water immersion objective lens (XLUMPlanFI 20x/0.95 W, Olympus). A band-pass filter (transmission at wavelength between 595 nm and 665 nm) and a long-pass filter (transmission at wavelength longer than 650 nm) are used to separate the CARS signal from the excitation beams and other nonlinearly generated light such as two-photon excited fluorescence. The pixel clock is extracted from the microscope, and is used as a time reference for two function generators that directly modulate the CW sources to achieve the desired pixel-on, pixel-off effect. Modulation speeds up to 2 MHz can be achieved.

We first characterize the pump. The average power of the pump is 200 mW. The measured spectrum of the pump is shown in Figure 2(a). The center wavelength and the bandwidth of the pump are 816.8 nm and 1.8 nm, respectively. The corresponding pulse width of the pump, deconvolved from the measured second-order interferometric autocorrelation trace [Figure 2(d)], is 1 ps (a deconvolution factor of 1.4 is used, assuming the pulse has a Gaussian profile).

We then characterized the Stokes beams (time-lens output) and the synchronization performance. The average power after modulation and compression is 400 mW in the nonresonant Stokes beam at 1056 nm and 400 mW in the resonant Stokes beam at 1063.6 nm. Both wavelengths have a spectral full width at half maximum (FWHM) of ~ 1.5 nm, as shown in Figures 2(b) and 2(c). For temporal profile characterization, we perform a cross-correlation between the time-lens output and the 100 fs pulse directly from the mode-locked Ti:Sa laser using collinear sum frequency generation in a beta barium borate (β -BBO) crystal of 0.5 mm thickness. Scanning the relative delay between the beams was achieved by tuning the RF delay between the electro-optical modulators and the Ti:Sa pulse train. As shown in Figures 2(e) and 2(f), the temporal FWHM of the two-wavelength time-lens output is 1.9 ps for both the resonant and nonresonant Stokes beams. To measure the relative timing jitter between the time-lens source and the 100 fs pulse from the mode-locked Ti:Sa laser, we record the sum frequency intensity fluctuation at the half-maximum of the cross-correlation trace [inset in Figures 2(e) and 2(f), sampled at 1 kHz]. The measured root-mean-square (RMS) timing jitters for resonant and nonresonant Stokes over a measurement time of 350 s are 44 and 50 fs, respectively, only a small fraction of the pulse widths and suitable for CARS imaging.

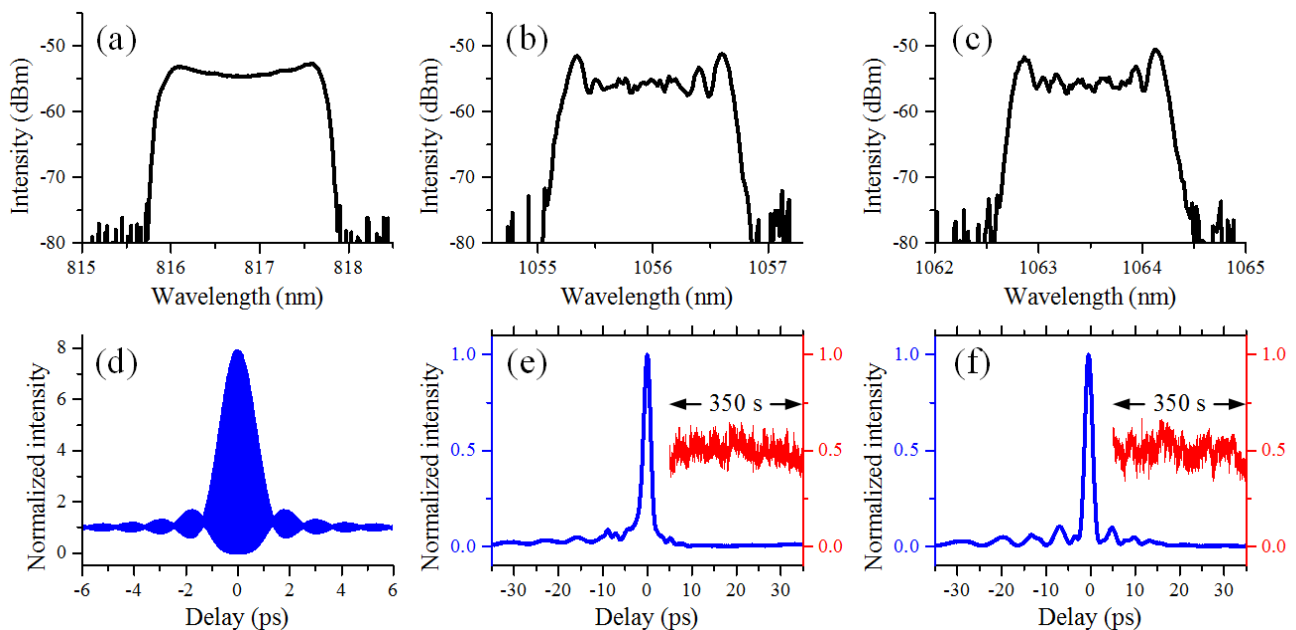


Figure 2. Characterization of the lasers for CARS imaging. (a) Spectrum of the pump laser. (b, c) Spectra of the time-lens source at ~ 1056 nm and ~ 1063.6 nm, respectively. (d) Second order interferometric autocorrelation of the pump laser. The de-convolved FWHM of the pulse is approximately 1 ps. (e) Second order cross-correlation trace between the 1.9 ps pulse at 1056 nm (b) and the 100 fs pulses from the mode-locked Ti:Sa laser. (f) Second order cross-correlation trace between the 1.9 ps pulse at 1063.6 nm (c) and the 100 fs pulses from the mode-locked Ti:Sa laser. The insets in (e) and (f) show the measured sum-frequency signal at the half-maximum of the cross-correlation traces over 350 s (sampled at 1 kHz).

2.3 Imaging results

To demonstrate the capabilities of the two-wavelength time-lens source for background-free CARS image, we performed CARS imaging of sebaceous glands in *ex vivo* mouse ear tissue. The microscope pixel clock and the time-lens source are synchronized to provide pixel-to-pixel control of the on- and off-resonance imaging. By alternating the two Stokes beams, the adjacent pixels in the image are excited by either the on-resonance beam or the off-resonance beam. Therefore, on- and off- Raman resonance imaging is achieved within one pixel dwell time ($\sim 2 \mu\text{s}$). As an example, CARS imaging of sebaceous glands in *ex vivo* mouse ear tissue at the CH_2 stretching frequency (2845 cm^{-1}) is shown [Figures 3(a)-3(d)]. In the experiment, the mode-locked Ti:Sa laser is tuned to 816.8 nm , the Stokes beam is tuned to 1063.6 nm (on resonance with the CH_2 stretching vibrational frequency at 2845 cm^{-1}), and the nonresonant Stokes beam is tuned to 1056 nm (off-resonance at 2773 cm^{-1}). The average power of the pump, resonant Stokes and nonresonant Stokes beams on the sample are 55 mW , 20 mW and 20 mW , respectively. In particular, the on-resonance image shown in Figure 3(a) has a strong CARS signal with nonresonant background, while the off-resonance image shown in Figure 3(b) has a weak CARS signal with the same nonresonant background. By a simple subtraction of on- and off-resonance images, background-free CARS images [Figure 3(c)] are obtained, with significantly improved contrast when compared to the original image without background subtraction [Figure 3(a)]. Figure 3(d) shows the image when the pump and Stokes beams do not overlap in time (a RF delay of 80 ps was introduced), proving that the signal is CARS and indicating that contributions (e.g., two-photon excited fluorescence, room light, laser leakage, etc.) other than the nonresonant background are negligible.

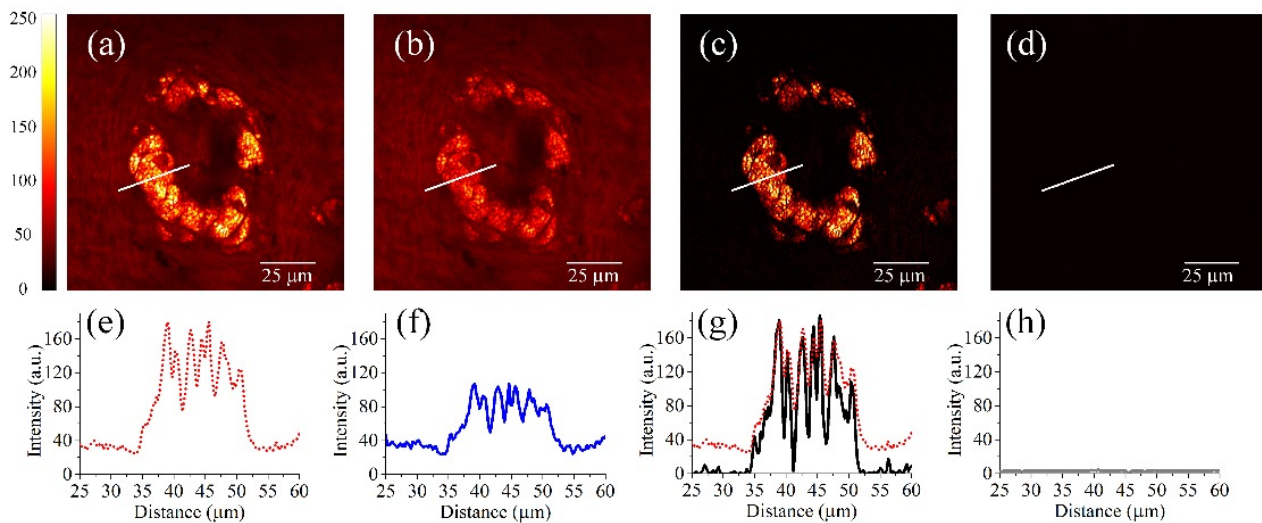


Figure 3. CARS images of sebaceous glands in *ex vivo* mouse ear tissue, with the source tuned to the CH_2 stretching frequency. 800×800 pixels, $2 \mu\text{s}/\text{pixel}$, no average. (a) Image formed from the on-resonant pixels (all odd columns). (b) Image formed from the off-resonant pixels (all even columns). (c) Image after the subtraction of the nonresonant background (b) from the resonant signal (a). Note that the brightness of the image is increased by ~ 2 times to match the brightness scale of (a). (d) Image taken when the pump and Stokes beams do not overlap in time (an RF delay of 80 ps was introduced). (e-h) show the corresponding intensity profiles along the lines indicated in the images (a-d). For comparison, the intensity profile in (a) (dashed red line) is also shown in (g).

CONCLUSION

In conclusion, we have experimentally demonstrated background free CARS imaging using a two-wavelength time-lens source. Two synchronized picosecond sources with hundreds of milliwatts of optical power were generated through time-lens pulse compression of CW lasers. Direct modulation of the CW lasers using the microscope pixel clock ensures

synchronization of image acquisition and the time-lens source, and enables real-time (pixel by pixel) subtraction of the nonresonant background in the CARS image. The demonstrated technique has the advantages of convenient synchronization to both the microscope pixel clock and the mode-locked laser in a robust, cost-effective, all-fiber configuration. While two wavelengths were demonstrated in this paper, it is relatively straightforward to include more wavelengths in the time-lens source. Multi-wavelength time-lens sources may provide an all-fiber, user-friendly alternative for background-free CARS imaging.

REFERENCES

- [1] A. Zumbusch, G. R. Holtom, and X. S. Xie, "Three-dimensional vibrational imaging by coherent anti-Stokes Raman scattering," *Phys. Rev. Lett.*, 82(20), 4142-4145 (1999).
- [2] J.-X. Cheng, and X. S. Xie, "Vibrational spectroscopic imaging of living systems: An emerging platform for biology and medicine," *Science*, 350(6264), aaa8870 (2015).
- [3] M. Duncan, J. Reintjes, and T. Manuccia, "Imaging biological compounds using the coherent anti-Stokes Raman scattering microscope," *Opt. Eng.*, 24(2), 242352-242352- (1985).
- [4] A. F. Pegoraro, A. D. Slepko, A. Ridsdale *et al.*, "Hyperspectral multimodal CARS microscopy in the fingerprint region," *J. Biophotonics*, 7(1-2), 49-58 (2014).
- [5] O. Burkacky, A. Zumbusch, C. Brackmann *et al.*, "Dual-pump coherent anti-Stokes-Raman scattering microscopy," *Opt. Lett.*, 31(24), 3656-3658 (2006).
- [6] F. Ganikhanov, C. L. Evans, B. G. Saar *et al.*, "High-sensitivity vibrational imaging with frequency modulation coherent anti-Stokes Raman scattering (FM CARS) microscopy," *Opt. Lett.*, 31(12), 1872-1874 (2006).
- [7] K. Wang, D. Zhang, K. Charan *et al.*, "Time-lens based hyperspectral stimulated Raman scattering imaging and quantitative spectral analysis," *J. Biophotonics*, 6(10), 815-820 (2013).